

Echelon: Two-Tier Malware Detection for Raw Executables to Reduce False Alarms

Anandharaju Durai Raju*

Ke Wang†

Abstract

Existing malware detection approaches suffer from a simplistic trade-off between false positive rate (FPR) and true positive rate (TPR) due to a single tier classification approach, where the two measures adversely affect one another. The practical implication for malware detection is that FPR must be kept at an acceptably low level while TPR remains high. To this end, we propose a two-tiered learning, called *Echelon*, from raw byte data with no need for hand-crafted features. The first tier locks FPR at a specified target level, whereas the second tier improves TPR while maintaining the locked FPR. The core of Echelon lies at extracting activation information of the hidden layers of first tier model for constructing a stronger second tier model. Echelon is a framework in that it allows any existing CNN based model to be adapted in both tiers. We present experimental results of evaluating Echelon by adapting the state-of-the-art malware detection model “Malconv” in the first and second tiers.

Keywords: cyber security, malware detection, static analysis, portable executable, activation trend

1 Introduction

Malware detection techniques like static and dynamic analysis deal with static codes and dynamic behaviors of malware, respectively. While dynamic analysis excels more than static methods, they are inefficient when used alone. Nowadays, both methods are used to complement each other’s advantages in form of hybrid analysis techniques [5]. In this paper, we focus on static, end-to-end deep neural network methods, to learn from raw byte sequence data with no need for hand-crafted features, similar to [14][7]. Another reason for considering raw byte sequences is that such data can be easily obtained without running a portable executable (PE) sample and with little data pre-processing effort.

The performance of malware detection software is defined by true positive rate (TPR) and false positive

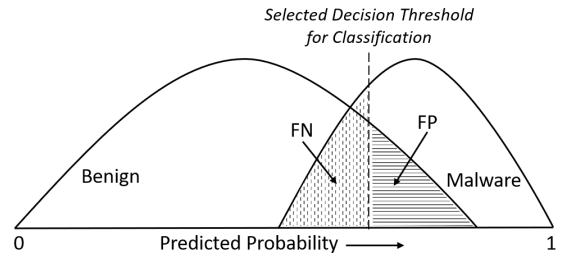


Figure 1: Trade-off between TP and FP

rate (FPR). TPR is the percentage of positive (malware) samples that are detected as positive, and FPR is the percentage of negative (benign) samples that are detected as positive. Using the confusion matrix, $TPR = \frac{TP}{TP+FN}$ and $FPR = \frac{FP}{FP+TN}$. The cybersecurity community is well aware of the importance of having a low FPR because a high FPR leads to many false alarms, which requires excessive manpower to manually investigate on each case, eventually reducing the confidence of using the system. On the other hand, there are different detection models that can be stacked together to catch FNs (i.e., malware files misclassified as benign) [22][5]. According to [13], it is essential to keep FPR at 1% or lower while TPR remains no less than 90%. However, achieving such performance is a challenge for traditional single tier classification, such as [7][20][14][8], which suffers from the simplistic TPR/FPR trade-off due to the decision threshold shown in Figure 1 - a reduced FPR is always at the expense of a lowered TPR (note $TPR = 1 - \frac{FN}{FN+TP} = 1 - FNR$).

To keep FPR at an acceptably low level while maintaining a high TPR, we propose the *locked FPR* requirement and a *two-tiered* solution called Echelon. Echelon learns the model at two tiers. The first tier locks a specified *target FPR* but may have a low TPR. The second tier is responsible for improving TPR while having no or little increase of FPR. With each tier having its own decision threshold, Echelon does not suffer from the simplistic trade-off of TPR/FPR that results due to a single decision threshold. Echelon is a framework in that it can convert an existing convolutional neural network (CNN) based model into

*aduraira@sfu.ca, Simon Fraser University, Canada

†wangk@sfu.ca, Simon Fraser University, Canada

two-tiered models by adapting it in both first and second tiers; the only assumption is that the CNN model has a max pooling layer followed by a fully connected network.

The challenge lies at learning a strong second tier model that must lock the target FPR achieved by the first tier while substantially increasing the overall TPR. We learn the second tier model through a novel *Activation Trend Identification (ATI)* mechanism. ATI focuses on the TN and FN samples of the first tier and identifies the PE sections that have high activations at the hidden layers of first tier model for either class but not both. Such high activation sections provide sharpened features to distinguish TN samples and FN samples in the second tier, thereby, correcting FNs of the first tier while introducing zero or little new FPs.

We further consider two enhancements for the above section-based approach. The first enhancement focuses on actual data regions within an identified PE section that yield high activations, instead of whole PE section. This restriction helps reduce the training data size in expensive Tier-2 training. The second enhancement incorporates PE section level semantics, in addition to activation data regions, for utilizing high level information modality offered by different PE sections.

As a proof of concept, we adapted the state-of-the-art CNN malware detection model, Malconv[14], into the first and second tiers of Echelon and evaluated it on real malware datasets. The study shows that a significant improvement of up to $\approx 5\%$ over Malconv's TPR is achievable while retaining FPR at target 0.1%. This improvement is obtained by the second tier over difficult samples that Malconv failed to learn and classify.

The rest of the paper is organized as follows. Section 2 reviews related works. In Section 3, a brief background on PE file format and the basic Malconv architecture are provided. Section 4 presents our two-tier Echelon framework, followed by the details of activation trend identification in Section 5 and the training algorithms in Section 6. Section 7 presents the datasets and experimental results. Finally, Section 8 concludes this study.

2 Related Work

We consider three categories of related works.

2.1 Based on Byte Sequences: Most works dealing with byte sequence data are based on neural networks. Raff et al[14] and Coull et al[4] are single-tiered approaches, which suffer from the simplistic TPR-FPR trade-off. They use raw bytes as base features and analyze hidden layer activations to showcase that deep neural networks could learn information similar to a malware analyst. The Malconv CNN model by [14] treats a

raw executable as a single byte sequence on its entirety, ignoring the PE section level semantics on multi-modal contents like image, code, etc., thus, loses the benefits of leveraging semantic information for better detection. [4] auto-extracted low-level 11-byte feature representations from (100KB) samples that resembles manually-derived features, whereas we use higher level PE section data from samples of size up to 1MB, as our automated feature representation for better generalization.

[7] proposed a simpler CNN based model for byte data performing similar to [14], and [22] proposed a hybrid framework with classic and deep learning models along with Malconv variants. Both suffer the same issue as described for [14]. [8] proposed a method for feature identification without expert domain knowledge. Their method completely ignores PE section level semantics of PE samples as they artificially re-scale the 1-D byte code to a fixed 10k bytes length using OpenCV library. Such lossy data compression is prone to over-fitting.

[9] showed that applying deep learning over disassembled raw binary content has merits in considering the semantic meaning of each byte. They used the PE section's characteristics instead of its binary content and used severely downsampled (32x32) malware image representations as input, which would corrupt PE semantics and would not be scalable for real world samples.

2.2 Based on Feature Extraction: Many works assume a vectorized feature space for input that require expensive domain knowledge based feature extraction. [20] and [17] use fixed size n-gram byte blocks as feature. While n-gram methods are useful, they are computationally expensive due to the enormous n-grams and might not cover long range dependencies that are important for our purpose, and they are prone to over-fitting, suffer extreme sparsity, and give diminished returns with more data[15]. [3] compared the performance of LightGBM model with Malconv model using features such as raw-byte histogram, byte-entropy histogram, etc. Other feature types include string-2D histogram [18], GIST-based binary textures [11], Markov n-grams' entropy rate [19], and structural byte entropy graphs [26]. Extracting such features needs specialized feature engineering pipelines.

2.3 Based on Multi Classifiers: Existing ensemble strategies use multi classifiers to improve classification accuracy [10], such as *Bagging*, *Boosting*, *Voting*, *Stacking*. In these methods, each weak learner provides additional information to derive an improved final classification. In contrast, our two tier Echelon is motivated by the specific malware detection requirement to enforce a target FPR while maximizing TPR, which cannot be

achieved by simply improving the general classification accuracy. In our two tier model, each tier is responsible for a different subset of prediction: the Tier-1’s prediction of the malware class (both TP and FP) is final; Tier-2’s purpose is to reclassify misclassified malwares to increase TPR. Such a split of prediction is very different from ensemble algorithms where each weak learner provides additional information to the final learner but does not make a final prediction.

Using n-grams, [2] proposed a multi-tier ensemble of meta-classifier ensembles and [28] proposed an ensemble of probabilistic neural networks. [1] and [6] used two classifiers in Tier-1 and one classifier in Tier-2, focusing on both FPs and FNs for feature selection in the Tier-2. These works address general prediction mismatches, instead of locking a target FPR and improving the TPR, and do not directly work with raw byte sequences, but rely on n-grams like feature extraction.

The two-level hierarchical associative classifier in [27] aims for high recall, i.e., TPR, in first level while optimizing precision in the next level. Their work lacks locking FPR at a target level, which is our focus, and their work requires API call based feature extraction.

Finally, there are false alarm reduction related works on anomaly detection [21] using network intrusion detection systems. Such works are very different from our malware detection scenario dealt here.

3 Background

We first briefly introduce the file format of PE samples and then, discuss shortly about Malconv [14] model that will be adapted as our Tier-1 model in the presentation.

Section Name	Description
.text	Comprises executable code
.data	Holds initialized application data
.rdata	Read-only data like strings, constants
.edata	Export directory for an application
.idata	Import directory & address table
.bss	Holds uninitialized application data
header	Information about other sections
.debug	Deugging related information
.reloc	Information on image relocations
.rsrc	Module resources like images & icons

Table 1: Typical sections in a PE sample

3.1 PE Samples: Windows Portable Executable (PE) is a Windows 32/64-bit file format used for DLLs, executable programs, etc. Here, we consider a broader level sub-area present in a PE file called “PE Section”,

that provides a logical and physical separation to different parts of the program contained in PE file, and also helps in loading the executable file into memory during execution. Table 1 contains the details of some PE sections that are prevalent in most PE samples. Other custom made sections may also be present. For example, there were more than 2,500 distinct PE section names found collectively across the samples in our datasets.

A lookup directory named “Section-Table”¹, located usually after Header data, lists meta information like the PE section’s names, its virtual size, and location - in the order of their relative virtual address (RVA). Further details about PE sections can be referred at [12]. There exists no uniformity in terms of a PE section’s presence, their sizes across samples, and the order in which they appear. Hence, treating PE byte sequence as a 2-D image like [25] will lose the PE semantics: a same pixel value will have the same intensity anywhere in an image, but a same byte value in a PE sample will have different meanings in different PE sections. While we focus on Windows PE, our work can be transferrable to other file formats such as Linux (ELF file format) based malware, which are on the rise recently.

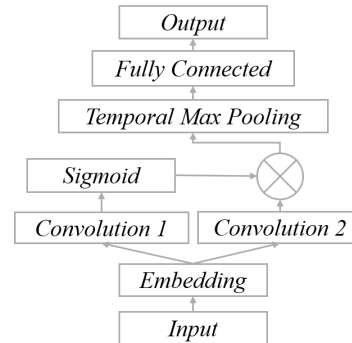


Figure 2: Architecture of Malconv

3.2 The Malconv Architecture: Our Echelon framework can adapt any CNN-based model with a max pooling followed by a fully connected network. We use Raff et al’s Malconv model by [14] for our presentation. The architecture of the Malconv model is illustrated in Figure 2. It maps input to an 8-dim embedding layer, which is then parallely fed into two 1-D convolutional layers, one of which is followed by a sigmoid layer. Both layer outputs are multiplied element-wise by coupling them to a gating mechanism, followed by a temporal max-pooling layer for obtaining the global maximums, that are fed into a fully connected layer to get final output. More details will be presented in Figure 4.

¹docs.microsoft.com/en-us/windows/win32/debug/pe-format

4 The Echelon Framework

4.1 Overview: The aim of Echelon is to obtain a better TPR while locking FPR at a specified level. It receives a user-specified target FPR as input along with a collection of labeled PE samples. Echelon adapts an existing CNN model and produces two models called Tier-1 model and Tier-2 model, that are trained sequentially to achieve the overall target FPR, and an overall TPR higher than what the Tier-1 model alone could achieve. While the Tier-1 model uses the adapted model, the Tier-2 model has a similar network architecture but is trained on a subset of the original training data and selected PE sections or data regions. The high level training flow in Echelon is shown in Figure 3. Each tier has a specific purpose in the whole malware detection process, described as follows.

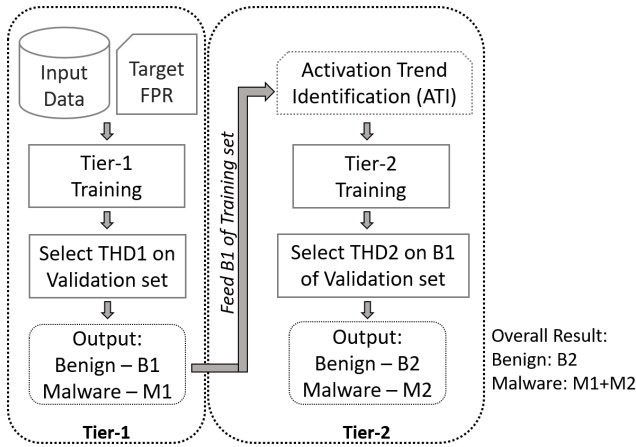


Figure 3: Echelon training flow.

4.2 Tier-1: We divide the labeled dataset into training, validation, and testing. Training the Tier-1 model is the same as training the adapted CNN model except that the decision threshold THD_1 is selected to comply with the given target FPR on the validation set. The validation set, not the training set, is needed to avoid overfitting. The Tier-1 model classifies the training set into $B1_{train}$ and $M1_{train}$, representing the subset of predicted benign samples and the subset of predicted malware samples, and similarly classifies the validation set into $B1_{val}$ and $M1_{val}$ sets. Note that generically $M1$ consists of true positives (TP_1) and false positives (FP_1), and $B1$ consists of true negatives (TN_1) and false negatives (FN_1). The compliance with the target FPR implies that the prediction for the samples in $M1$ is final, but $B1$ may contain excessive actual malware samples, i.e., FNs, which the Tier-1 model failed to learn and classify due to the target FPR compliance.

4.3 Tier-2: The objective of Tier-2 training is to correct the FNs in $B1$, i.e., reclassify them into malware while ensuring that the overall FPR of the two tiers together does not exceed the target FPR. Two ideas contribute to our Tier-2 training. First, Tier-2 training focuses on $B1_{train}$, i.e., the training samples classified as benign by Tier-1. Second, Tier-2 training focuses on “biased” PE sections whose hidden layer activation in the Tier-1 model shows a strong bias for positive vs negative samples in $B1_{train}$, thereby helping in capturing FNs in $B1$ while retaining TNs. Biased PE sections are identified by **Activation Trend Identification (ATI)** presented in the next section.

To preserve the target FPR, the decision threshold for Tier-2 model, THD_2 , is selected to be the minimum such that the overall FPR (Equation 4.1) of the two tiers on $B1_{val}$ is no more than the target FPR. Tier-2 model splits $B1_{val}$ into $B2_{val}$ and $M2_{val}$, where $B2_{val}$ consists of TN_2 and FN_2 , and $M2_{val}$ consists of TP_2 and FP_2 . The *overall FPR* on the validation set is the percentage of negative samples that are predicted as positive by either Tier-1 model or Tier-2 model:

$$(4.1) \quad Overall_FPR = \frac{FP_1 + FP_2}{FP_1 + FP_2 + TN_2}$$

The *overall TPR* is the percentage of positives that are predicted as positive by either Tier-1 or Tier-2 model:

$$(4.2) \quad Overall_TPR = \frac{TP_1 + TP_2}{TP_1 + TP_2 + FN_2}$$

These metrics are similarly defined for testing set.

4.4 Prediction: To classify an unlabeled sample x , we apply the two models sequentially, similar to classifying a validation sample. If the Tier-1 model predicts x as malware, i.e., belonging to $M1$, the prediction is final. If the Tier-1 predicts x as benign, i.e., belonging to $B1$, we apply Tier-2 model to predict the final label of x , using only the biased PE sections in x .

Next, we discuss how biased PE sections are identified using hidden layer information of the Tier-1 model.

5 Activation Trend Identification (ATI)

The functionality of ATI is to identify the PE sections with a strong activation bias in the two classes. To explain this functionality, we zoom-in the Malconv network in Figure 4 as the adopted model for our Tier-1 model. While there are possibly multiple hidden layers in the Tier-1 model, only the maximum activation that passes through the max pooling is visible to the subsequent fully connected network. Therefore, we shall focus on the *top activations* that survived the max pooling and identify the PE sections that yielded

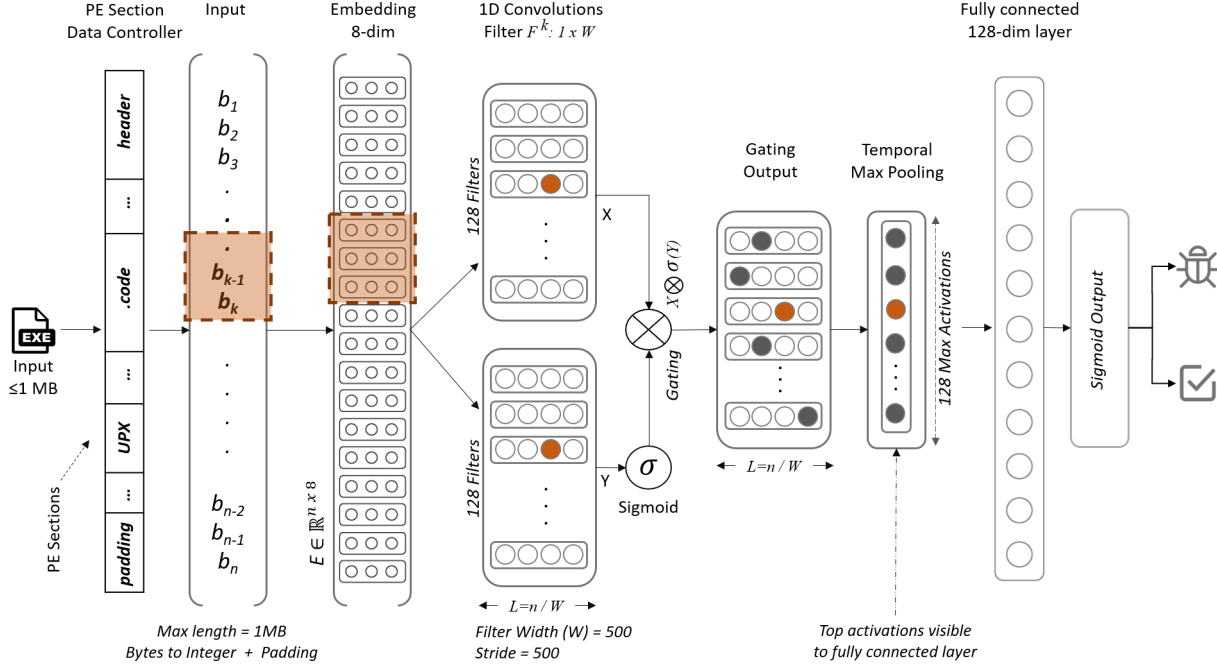


Figure 4: A top activation value generated by max pooling in the Tier-1 model (Malconv). The highlighted places represent the intermediate data responsible for generating the top activation at various stages of the model.

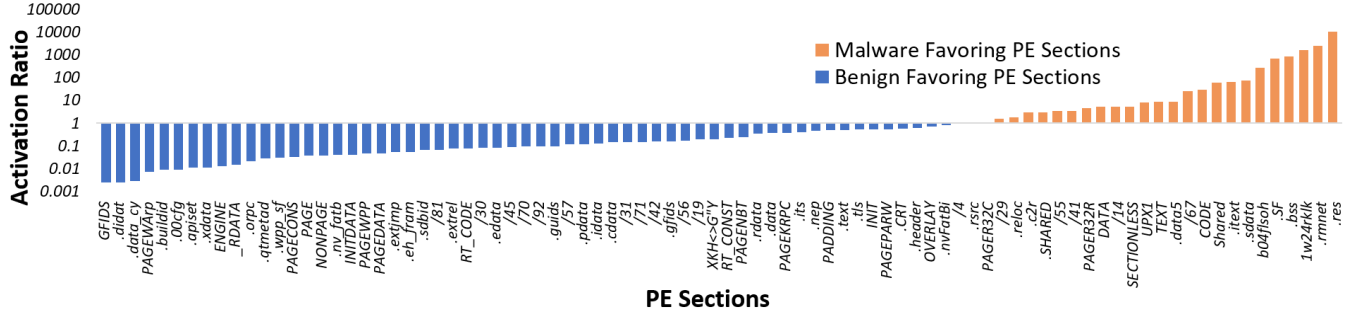


Figure 5: Histogram of AR_s for some PE sections in DS1 dataset.

top activations at vastly different rates for benign and malware classes, to train the Tier-2 model.

Figure 4 illustrates the tracing of a PE section responsible for generating a top activation. From left, we have the byte sequence input, a controller to filter biased PE section data, embedding, and convolution layers with 128 filters. Each filter has the convolutional width W and produces $L = n/W$ activation values on a sample of n bytes. The tracing goes in the opposite direction starting from a top activation value after max pooling. The highlighted places show the corresponding data of the top activation at various stages of the model, which traces back to a portion of W byte input sequence. This relationship allows us to identify the PE section containing these W bytes for each top activation,

with the help of a python library called “pefile” that provides address offsets of PE sections in a PE sample.

Let S be the set of all distinct PE section names. Consider a PE section name $s \in S$ and the benign class denoted by C^- . Let n_{C^-} be the total number of C^- samples in $B1_{train}$, k_s be the number of top activations produced by s in the k^{th} sample in $B1_{train}$. We define the *mean benign activation trend* of s as the average number of top activations of s in all the $B1_{train}$ samples:

$$(5.3) \quad T_s^- = \frac{\sum_{k=1}^{n_{C^-}} k_s}{n_{C^-}}$$

Intuitively, T_s^- measures the activation level of the sections named s among benign training samples. Sim-

ilarly, T_s^+ denotes *mean malware activation trend* for sections named s in the malware class C^+ . We define the *activation ratio* or AR, for each s in S as,

$$(5.4) \quad AR_s = T_s^+ / T_s^-$$

We are interested in the section names s among S with AR_s far away from 1, that is, s produces far more top activation in benign samples than in malware samples, or vice versa. This difference makes s an ideal candidate for discriminating between the two classes. Figure 5 shows the histogram for AR_s of some PE section names found in our dataset, sorted by increasing AR_s with blue for $AR_s < 1$ and orange for $AR_s > 1$. Those sections with a large blue bar or orange bar are biased towards benign or malware, therefore, are useful for training the Tier-2 model. Note that large bars of both colors are needed because we need to keep new FPs low while finding many new TPs in Tier-2.

Let S_{bias} denote a set of section names from S that have a large bar of either color, where “large” can be defined by some cut-off value either on the bar size or on the number of section names to be included from both sides of the AR_s histogram. In our algorithms below, this cut-off is treated as a hyperparameter for Tier-2 training and is searched using the B1 of validation set.

6 Training Algorithms

We now put the above idea in several implementations, where each next implementation improves the previous one by either reducing the training data size or capturing more information for better accuracy.

6.1 Section-based: This is the straightforward implementation, summarized in Algorithm 1. Tier-1 training is as in Section 4.2. The Tier-2 model’s architecture is similar to that of Tier-1 model. There are two key differences in Tier-2 training: it uses $B1_{train}$ as the training set and keeps only the sections with their names in S_{bias} for Tier-2 training (by removing other PE sections’ data from the sample and concatenating remaining S_{bias} section data after padding them to the nearest multiple of the filter size W). The same restriction on S_{bias} will apply to the validation set and future prediction. The decision threshold THD_2 for Tier-2 model is selected to maximize the TPR on $B1_{val}$ subject to the constraint that the overall FPR is no more than the target FPR. Finally, the Tier-1 model and the best Tier-2 model, together with their THD_1 and THD_2 , are returned. Note that Tier-2 training is more time-consuming than Tier-1 training due to the search for optimal S_{bias} through multiple cut-off values. There is a trade-off between the number of cut-offs considered and Tier-2 training time.

Algorithm 1 Two-Tier Training Process

Tier-1 Training

- 1: Train Tier-1 model on training data
- 2: Find THD_1 that meets the target FPR on validation set
- 3: Let $B1_{train}$ and $B1_{val}$ be the subsets of training set and validation set predicted as benign
- 4: Compute AR_s for each PE section s over $B1_{train}$

Tier-2 Training

- 5: **for all** cut-offs for S_{bias} **do**
 - 6: Let S_{bias} = PE section names selected by cut-off
 - 7: Train Tier-2 model using $B1_{train}$ ’s S_{bias} data
 - 8: Find THD_2 with highest TPR on $B1_{val}$ without violating the target FPR by overall FPR
 - 9: Set $Best$ as Tier-2 model with highest TPR on $B1_{val}$
 - 10: **end for**
 - 11: Return Tier-1 and $Best$ Tier-2 models with respective THD_1 and THD_2
-

6.2 Block-based: In section-based implementation, the entire data of a S_{bias} PE section is kept to train the Tier-2 model even though a small portion may be responsible for producing the top activation for Tier-1 model. In the block-based implementation, for each top activation from the Tier-1 model, we keep only the portion of data, called a *block*, with a size equal to W , which actually generates the top activation. We remove the rest of the bytes in that PE section and concatenate the remaining byte blocks. Then Tier-2 model is trained using such a compressed version of $B1_{train}$ samples. The rest of Algorithm 1 remains unchanged. With our datasets and $W = 500$, this compression leads to $\approx 94\%$ data reduction compared with $B1_{train}$ ’s original size. Similar compression is performed for validation and testing/future sets.

6.3 Semantic-Aware: In Figure 4, beyond the temporal max pooling layer of block-based implementation, the subsequent fully connected network training is oblivious as to which PE section triggered the top activation. As a result, similar activation values produced by different PE sections have no discriminating power of two classes, even though their PE section names, which represents different semantics, could discriminate the two classes. To address this issue, we assemble a vector of size same as the activation vector, to provide the corresponding section name for each top activation to the subsequent fully connected network. In Figure 4, this means that the total input size of the fully connected neural network is 256, instead of 128.

7 Evaluation

We provide evidences for our 2-tier approach based on experiments adapting Malconv[14] model. All exper-

iments were based on the (80:20):20 splits of (Training: Validation): Testing. We set the convolution filter width $W = 500$ as used by [14] and used a training batch size of 64 samples. S_{bias} contains an equal number of PE section names from both ends of the activation ratio histogram like in Figure 5, where the number is treated as a hyperparameter in Tier-2 training. All the experiments were run on 4x16GB P100 GPUs, with a limit of 200 epochs, an early stopping patience set to 5 epochs, and a learning rate of 0.001 using Adam optimizer.

Data	Category			Sample Size (MB)		
	Benign	Malware	Total	Min	Max	Avg
DS1	102,275	102,272	204,547	0.0006	1	0.41
DS2	80,565	51,841	132,406	0.0007	1	0.33

Table 2: Dataset Distribution

7.1 Datasets: We prepared two datasets of different ratio of the two classes, described as DS1 and DS2 in Table 2. DS1 was created with $n_{C^+} \approx n_{C^-}$, similar to [14][4], and DS2 with $n_{C^-} > n_{C^+}$. DS1 comprises the malware corpus provided by VirusTotal[24] falling in the range of Jan to Mar 2019, and DS2 comprises malware corpus from VirusShare[23], from sets 350 to 356. While it is possible to get these datasets from [24][23], their policy², however, does not allow us to release their datasets. The benign samples were collected from Windows machines with fresh Windows OS installation of versions 7, 8, and 10. Only the samples with size ≤ 1 MB were selected from the collected corpus to create the datasets. DS1 and DS2 contained an overall of 2,678 and 2,220 distinct PE section names respectively.

We report the performance on TPR and FPR using 5-fold CV with the target FPR set at 0.1% (see a discussion on setting a stringent target FPR in Introduction). An important point to note is that the reported TPR/FPR performance is expected to hold when applying the models to future data where the ratio of the two classes may be different from our testing set. This is because, unlike Accuracy and Precision metrics, TPR measures the probability of detecting malware (positive) samples within the malware class, and this probability is determined by the model trained, not by the relative size of the two classes in testing/future data. The same argument applies to FPR. Hence, the reported TPR/FPR performance will hold on any testing/future sets that have a different $n_{C^-} : n_{C^+}$ class ratio from the one used here. Indeed, this is confirmed on testing sets with class ratios 1:1, 5:4, 5:3, 5:2, 5:1, and 10:1.

²support.virustotal.com/hc/en-us/articles/115002168385-Privacy-Policy

7.2 Results for DS1 dataset: The results for DS1 testing set are reported in Table 3. The first three rows are the three implementations of the 2-tier framework in Section 6. The next three are the counterparts that use all sections in S in Tier-2 training instead of only those in S_{bias} . We compare our overall performance with independent results of three state-of-the-art works: Malconv [14], as it is chosen as our Tier-1, Krčál *et al* [7], a byte sequence model similar to Malconv but claimed to be performing better, and CNN-Xgboost [16], a multi-classifier approach combining CNN for dealing with sequence data, and Xgboost for boosting accuracy.

The columns for Tier-1 represent TPR and FPR of Tier-1 only, which is also the result of Malconv when forced to meet the target FPR. The columns for overall results represent the overall TPR and FPR of the 2-tier approach, therefore, the difference is the contribution of the Tier-2 model over the single tier model. The next set of columns give the New TPs and FPs produced by Tier-2, the data reduction in terms of biased sections in $B1_{train}$, and the training time of Tier-1 and Tier-2. Several observations can be drawn from Table 3.

Observation 1: Compared to the counterparts of using all sections, focusing on data of the S_{bias} sections (such as CODE, UPX1, etc.) helped lock the FPR over the “unseen” Testing set. This is because the S_{bias} sections exhibited a larger bias between benign and malware classes (i.e., their AR_s are far away from 1). On the other hand, the PE sections with AR_s close to 1 could cause the FPR instability on unseen samples as they are poor at discriminating the two classes. This explains why the target FPR was not met on the testing set by the implementations using all sections, though it was enforced on the validation set during training. This comparison reveals the effectiveness of S_{bias} sections.

Observation 2: The block-based and semantic-aware implementations achieve 3.85% and 4.94% improvement in TPR over the Tier-1 respectively, while retaining the FPR within the target 0.1%. This improvement is explained by the new TPs and new FPs columns. For example, Tier-2 of the block-based implementation has new TPs about 787, at the expense of a small increase of only 3 FPs. Due to only a small increase of FP, the target FPR continues to be satisfied whereas TPR increases from 89.03% to 92.88%. The semantic-aware implementation captures an additional ≈ 223 TPs at an even smaller cost of 2 FP, thanks to the section name information. The detailed confusion matrix on semantic-aware’s results is given in Table 5.

Observation 3: The semantic-aware and block-based reports well-reduced time consumption in Tier-2 training compared to section-based. For all implementations, time spent on Tier-2 depends on the step size

Implementation Type	Tier-1 TPR%	Tier-1 FPR%	Overall TPR%	Overall FPR%	New TPs in Tier-2	New FPs in Tier-2	#. of S_{bias} sections used	Tier-1+Tier-2 Training (hrs)
Section-based 2-tier	89.03	0.08	92.47	0.12	702.3	7.1	306.4/621	8.7+ 27.1
Block-based 2-tier	89.03	0.08	92.88	0.10	787.8	3.3	306.4/621	8.7+ 16.5
Semantic-aware 2-tier	89.03	0.08	93.97	0.09	1010.4	2.1	306.4/621	8.7+ 15.4
Section-based using all sections	89.03	0.08	92.56	4.66	722.7	936.6	621/621	8.7+ 31.4
Block-based using all sections	89.03	0.08	92.71	3.01	754.7	599.2	621/621	8.7+ 18.2
Semantic-aware using all sections	89.03	0.08	92.76	2.87	762.9	570.6	621/621	8.7+ 18.1
Malconv [14]	-	-	89.03	0.08	-	-	-	8.7
Krčál <i>et al</i> [7]	-	-	86.22	0.09	-	-	-	13.2
CNN-Xgboost [16]	-	-	93.90	2.20	-	-	-	9.2

Table 3: 5-Fold CV results on hold-out testing set over DS1 dataset @ 0.1% target FPR. Adapted model: Malconv

Implementation Type	Tier-1 TPR%	Tier-1 FPR%	Overall TPR%	Overall FPR%	New TPs in Tier-2	New FPs in Tier-2	#. of S_{bias} sections used	Tier-1+Tier-2 Training (hrs)
Section-based 2-tier	86.55	0.09	89.91	0.13	351.7	6.2	198.9/489	6.5+ 13.1
Block-based 2-tier	86.55	0.09	90.87	0.10	445.3	2.3	198.9/489	6.5+ 7.6
Semantic-aware 2-tier	86.55	0.09	91.41	0.09	503.9	1.3	198.9/489	6.5+ 7.3
Section-based using all sections	86.55	0.09	89.51	5.39	308.4	853.5	489/489	6.5+ 15.3
Block-based using all sections	86.55	0.09	90.76	4.87	436.9	770.1	489/489	6.5+ 9.8
Semantic-aware using all sections	86.55	0.09	90.78	4.85	438.1	766.2	489/489	6.5+ 9.5
Malconv [14]	-	-	86.55	0.09	-	-	-	6.5
Krčál <i>et al</i> [7]	-	-	81.70	0.10	-	-	-	9.1
CNN-Xgboost [16]	-	-	89.13	1.24	-	-	-	6.9

Table 4: 5-Fold CV results on hold-out testing set over DS2 dataset @ 0.1% target FPR. Adapted model: Malconv

DS1 Dataset	TN	FP	FN	TP	DS2 Dataset	TN	FP	FN	TP
Tier-1	-	16.4	-	18210.2	Tier-1	-	13.9	-	8973.5
Tier-2	20436.5	2.1	1233.4	1010.4	Tier-2	16097.8	1.3	890.6	503.9
Overall	20436.5	18.5	1233.4	19220.6	Overall	16097.8	15.2	890.6	9477.4

Table 5: Averaged Confusion matrix of 5-fold CV for Semantic-aware implementation. The number of benign and malware samples in DS1 testing set are 20,455 and 20,454 respectively, and in DS2 are 16,113 and 10,368 respectively. Note that Tier-1 has only FP and TP because only the prediction of positive class is final.

of the AR_s cut-off hyperparameter, which is set to 2% here. This time can be further reduced by increasing the step size, i.e., reducing number of cut-offs considered.

Observation 4: Our methods outperform all the external algorithms. Within external algorithms, Malconv’s individual performance is better than the rest. Malconv and Krčál *et al* report 89.03% and 86.22% TPR respectively when forced to meet the target FPR. CNN-Xgboost [16] results are not extrapolated, as it failed to meet the target FPR. Krčál *et al*’s model performed poorly on our dataset because they use a combination of local max-pooling and global average-pooling, that are easily influenced by noisy bytes in the input than global (temporal) max-pooling.

7.3 Results for DS2 dataset: The results on DS2 with target FPR as 0.1%, are found in Table 4. Here, semantic-aware has achieved 4.86% improvement over the Tier-1’s TPR, while keeping overall FPR at 0.09%, which is within the target FPR. The Tier-1 TPR

and overall TPR are relatively lower than that on the balanced DS1, as the model must learn to inhibit new FP occurrences wherein the training set’s benign population is more. Again, [16] failed to meet target FPR and [7] reported a lower TPR than Malconv’s.

8 Conclusion

High false alarms (i.e., FPR) lead to excessive manpower investigation and reduction of confidence in using the malware detection system. Traditional single tier learning suffers from the simplistic trade-off between TPR and FPR due to a single decision threshold. The proposed Echelon addresses this issue with two-tiered learning where the first tier locks FPR at a target level and the second tier improves TPR by learning from activation information of TN and FN samples at the hidden layers of the first tier. Echelon aims to be a general framework by allowing to adapt an existing CNN model in both tiers. Experimental evaluations

on samples collected from benchmark sources supported the design goals of Echelon. With PE sections as an automated byte-sequence feature representation, it also serves to improve the attribution of PE sections towards final classification outcomes.

9 Acknowledgements:

We acknowledge Ibrahim AbuAlhaol, Yang Zhou, and Huang Shengqiang for their valuable review and feedback for our work.

References

- [1] J. ABAWAJY AND A. KELAREV, *Iterative classifier fusion system for the detection of android malware*, IEEE Transactions on Big Data, (2017).
- [2] J. H. ABAWAJY, A. KELAREV, AND M. CHOWDHURY, *Large iterative multitier ensemble classifiers for security of big data*, IEEE Transactions on Emerging Topics in Computing, 2 (2014), pp. 352–363.
- [3] H. S. ANDERSON AND P. ROTH, *Ember: an open dataset for training static pe malware machine learning models*, arXiv preprint arXiv:1804.04637, (2018).
- [4] S. E. COULL AND C. GARDNER, *Activation analysis of a byte-based deep neural network for malware classification*, in 2019 IEEE Security and Privacy Workshops (SPW), IEEE, 2019, pp. 21–27.
- [5] A. DAMODARAN, F. DI TROIA, C. A. VISAGGIO, T. H. AUSTIN, AND M. STAMP, *A comparison of static, dynamic, and hybrid analysis for malware detection*, Journal of Computer Virology and Hacking Techniques, 13 (2017), pp. 1–12.
- [6] R. ISLAM AND J. ABAWAJY, *A multi-tier phishing detection and filtering approach*, Journal of Network and Computer Applications, 36 (2013), pp. 324–335.
- [7] M. KRČÁL, O. ŠVEC, M. BÁLEK, AND O. JAŠEK, *Deep convolutional malware classifiers can learn from raw executables and labels only*, <https://openreview.net/forum?id=HkHrmM1PM>, (2018).
- [8] Q. LE, O. BOYDELL, B. MAC NAMEE, AND M. SCANLON, *Deep learning at the shallow end: Malware classification for non-domain experts*, Digital Investigation, 26 (2018), pp. S118–S126.
- [9] D. G. LLAURADO, *Convolutional neural networks for malware classification*, Universitat Politècnica de Catalunya, Barcelona, (2016).
- [10] Y.-B. LU, S.-C. DIN, C.-F. ZHENG, AND B.-J. GAO, *Using multi-feature and classifier ensembles to improve malware detection*, Journal of CCIT, 39 (2010), pp. 57–72.
- [11] L. NATARAJ, V. YEGNESWARAN, P. PORRAS, AND J. ZHANG, *A comparative assessment of malware classification using binary texture analysis and dynamic analysis*, in Proceedings of the 4th ACM Workshop on Security and Artificial Intelligence, 2011, pp. 21–30.
- [12] M. PIETREK, *Peering inside the pe: A tour of the win32 portable executable file format - byte-pointer.com/resources/pietrek_peering_inside_pe.htm*, 1994.
- [13] A. A. POLYAKOV AND R. BIKKULA, *Mitigating false positives in malware detection*, May 6 2014. US Patent 8,719,935.
- [14] E. RAFF, J. BARKER, J. SYLVESTER, R. BRANDON, B. CATANZARO, AND C. K. NICHOLAS, *Malware detection by eating a whole exe*, in Workshops at the Thirty-Second AAAI Conference on Artificial Intelligence, 2018.
- [15] E. RAFF, R. ZAK, R. COX, J. SYLVESTER, P. YACCI, R. WARD, A. TRACY, M. MCLEAN, AND C. NICHOLAS, *An investigation of byte n-gram features for malware classification*, Journal of Computer Virology and Hacking Techniques, 14 (2018), pp. 1–20.
- [16] X. REN, H. GUO, S. LI, S. WANG, AND J. LI, *A novel image classification method with cnn-xgboost model*, in International Workshop on Digital Watermarking, Springer, 2017, pp. 378–390.
- [17] I. SANTOS, Y. K. PENYA, J. DEVESA, AND P. G. BRINGAS, *N-grams-based file signatures for malware detection.*, ICEIS (2), 9 (2009), pp. 317–320.
- [18] J. SAXE AND K. BERLIN, *Deep neural network based malware detection using two dimensional binary program features*, in 2015 10th International Conference on Malicious and Unwanted Software (MALWARE), IEEE, 2015, pp. 11–20.
- [19] M. Z. SHAFIQ, S. A. KHAYAM, AND M. FAROOQ, *Embedded malware detection using markov n-grams*, in International conference on detection of intrusions and malware, and vulnerability assessment, Springer, 2008, pp. 88–107.
- [20] S. M. TABISH, M. Z. SHAFIQ, AND M. FAROOQ, *Malware detection using statistical analysis of byte-level file content*, in Proceedings of the ACM SIGKDD Workshop on CyberSecurity and Intelligence Informatics, ACM, 2009, pp. 23–31.
- [21] A. B. VARUN CHANDOLA AND V. KUMAR, *Anomaly detection: A survey*, ACM Computing Surveys, (2009).
- [22] R. VINAYAKUMAR, M. ALAZAB, K. SOMAN, P. POORNACHANDRAN, AND S. VENKATRAMAN, *Robust intelligent malware detection using deep learning*, IEEE Access, 7 (2019), pp. 46717–46738.
- [23] VIRUSSHARE, *Malware repo - <https://virusshare.com/>*.
- [24] VIRUSTOTAL, *Malware repo - <https://virustotal.com>*.
- [25] M. WAGNER, F. FISCHER, R. LUH, A. HABERSON, A. RIND, D. A. KEIM, AND W. AIGNER, *A survey of visualization systems for malware analysis*, in Eurographics Conference on Visualization (EuroVis), 2015, pp. 105–125.
- [26] G. XIAO, J. LI, Y. CHEN, AND K. LI, *Malfcs: An effective malware classification framework with automated feature extraction based on deep convolutional neural networks*, Journal of Parallel Computing, (2020).
- [27] Y. YE, T. LI, K. HUANG, Q. JIANG, AND Y. CHEN, *Hierarchical associative classifier (hac) for malware de-*

tection from the large and imbalanced gray list, Journal of Intelligent Information Systems, 35 (2010), pp. 1–20.

- [28] B. ZHANG, J. YIN, J. HAO, D. ZHANG, AND S. WANG, *Malicious codes detection based on ensemble learning*, in International conference on autonomic and trusted computing, Springer, 2007, pp. 468–477.

Echelon: Two-Tier Malware Detection for Raw Executables to Reduce False Alarms - **Supplementary Material**

Anandharaju Durai Raju*

Ke Wang†

1 TPR/FPR Trend:

Generally, all the section-based, block-based and semantic-aware implementations, follow the principle that, the convolution filter width W of Tier-2 is same the W for Tier-1. Specifically, the data reduction in section-id aware and block-based implementations depend on the block-size that is directly controlled by the filter width W . [1] recommended to set filter width in powers of 2, since PE compilers tend to align the beginnings of PE sections within PE sample to multiples of powers of two such as 4096.

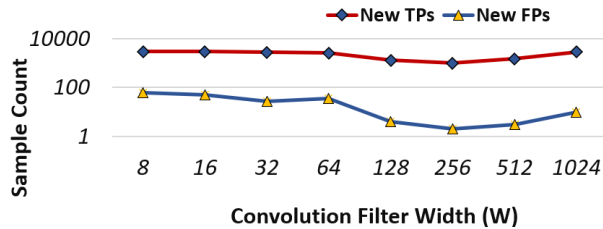


Figure 1: Section-ID Aware implementation: Trend of new TPs/FPs in Tier-2 for different W on DS1 dataset.

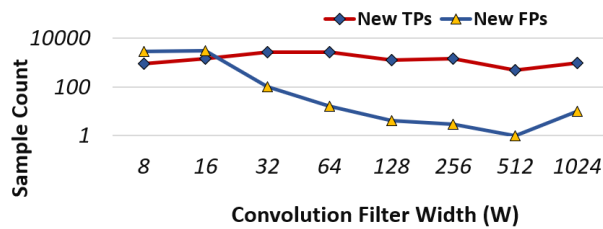


Figure 2: Section-ID Aware implementation: Trend of new TPs/FPs in Tier-2 for different W on DS2 dataset.

Figures 1 and 2 give the section-id aware implementation results of variation in new TPs/FPs introduced in Tier-2 for different W over DS1 and DS2 respectively. The filter widths such as 8, 16 failed to provide enough learnable information to Malconv model, making it to overfit on training data. On the other hand, very large

filter widths like 1024 tend to carry noisy information that in turns leads to increased FPR in Tier-2. The optimal block-size found for DS1 is 256 and DS2 is 512.

2 Boosting bound:

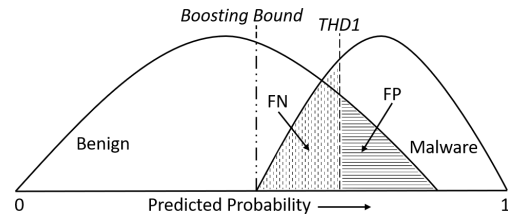


Figure 3: Boosting bound - Samples with output probability less than boosting bound will not be part of B1 set

Compared to the training set in Tier-1, the distribution of benign and malware samples in the training set for Tier-2, i.e., B_1 , is more imbalanced, i.e., $n_{C^+} \ll n_{C^-}$, because THD_1 was set favoring the lowest possible FPR. In Figure 3, B_1 is the set of samples that are on the left side of THD_1 , which contains far more benign samples than malware samples, making the Tier-2 training more challenging. To deal with this imbalanced distribution, we can exclude all samples from B_1 that are on the left side of the *boosting bound* in Figure 3, which is set to the lowest predicted malware probability of any malware sample over validation set. The reduced B_1 contains only the samples with predicted probability of malware class within the range of boosting bound and THD_1 , which is now more balanced in the two classes, and benefits in speeding up Tier-2 training.

With boosting bound, the following modification is needed for predicting an unlabeled sample. Before applying Tier-2 model, we first check if the predicted probability of malware class is less than boosting bound, if yes, the sample is predicted as benign, otherwise, Tier-2 model is applied to the sample to determine its class.

*aduraira@sfu.ca, Simon Fraser University, Canada

†wangk@sfu.ca, Simon Fraser University, Canada

3 Class Population Ratio:

We make use of TPR and FPR as primary evaluation metrics in our study. It is interesting to examine whether our objective of locking FPR and maximizing TPR evaluated on a testing set, will hold on future testing sets (real data) under the constraint of same class distribution but with varying benign to malware class population ratio.

Here, we denote class population as the number of samples drawn from a particular class, and class distribution as sample similarity.

Essentially for a given classifier, TPR and FPR set during training holds even when a different future testing set with different class ratio from that of the actual testing set, is used. Because FPR and TPR are determined by the classifier, not by the testing set. The key point here is that a given classifier is not affected by the choice of testing set.

By definition of TPR (Recall) and FPR, the portion of samples involved are relative to one class under consideration and are independent of the relative population size of the two classes. In other words, FPR and TPR do not depend on the change in the relative size of malware and benign samples in the testing data and the real data. With this observation, we can say that the FPR and TPR performance achieved on a more balanced data will hold on a less balanced real data, provided that both data are sampled from the same distribution. A set of tests done with different testing sets with different class ratio ($n_{C-} : n_{C+}$), such as 5:1, 10:1, etc., confirmed the same by resulting in similar TPR-FPR performance.

But other metrics such as Precision: $TP/(TP+FP)$ and Accuracy $(TP+TN)/(TP+TN+FP+FN)$, depends on the relative sizes of malware and benign samples because the underlying TP and FP depend on the two different class sizes. For instance, in case of Precision, by increasing the size of malware files, we have a larger TP and unchanged FP, therefore, a larger $TP/(TP+FP)$. Therefore, though recall does not depend on the relative class size, precision and accuracy does.

References

- [1] M. KRČÁL, O. ŠVEC, M. BÁLEK, AND O. JAŠEK, *Deep convolutional malware classifiers can learn from raw executables and labels only*, <https://openreview.net/forum?id=HkHrmM1Pm>, (2018).